Bica, Marian; Koivunen, Visa

Radar Waveform Optimization for Target Parameter Estimation in Cooperative Radar-Communications Systems

Published in:
IEEE Transactions on Aerospace and Electronic Systems

DOI:
10.1109/TAES.2018.2884806

Published: 01/10/2018

Document Version
Peer reviewed version

Please cite the original version:
Bica, M., & Koivunen, V. (2018). Radar Waveform Optimization for Target Parameter Estimation in Cooperative Radar-Communications Systems. *IEEE Transactions on Aerospace and Electronic Systems*, *55*(5), 2314 - 2326. https://doi.org/10.1109/TAES.2018.2884806

Radar Waveform Optimization for Target Parameter Estimation in Cooperative Radar-Communications Systems

Marian Bică, *Member, IEEE,* and Visa Koivunen, *Fellow, IEEE,*

***Abstract*—The coexistence between radar and communications systems has received considerable attention from the research community in the past years. In this paper, a radar waveform design method for target parameter estimation is proposed. Target time delay parameter is used as an example. The case where the two systems are not co-located is considered. Radar waveform optimization is performed using statistical criteria associated with estimation performance, namely Fisher Information (FI) and Cramér-Rao Bound (CRB). Expressions for FI and CRB are analytically derived. Optimization of waveforms is performed by imposing constraints on the total transmitted radar power, constraints on the interference caused to the communications system, as well as constraints on the Subcarrier Power Ratio (SPR) of the radar waveform. The frequency domain SPR is different than the Peak to Average Power Ratio (PAPR) which is computed in time domain. It is shown, using simulation results, that the proposed optimization strategies outperform other strategies in terms of estimation error. It is also shown that the SPR constraint reduces the delay domain ambiguities.**

***Index Terms*—spectrum sharing, coexistence, cooperation, multicarrier radar, communications systems, parameter estimation, agile radar, waveform optimization, power allocation**

I. Introduction

THE need for spectrum sharing and coexistence among radar and wireless communications systems was pointed out in [1]. Proposals for changing spectrum regulations have already been made by FCC in the US [2]. The coexistence problem has received a lot of attention from the research community in the recent years due to a considerable number of wireless systems that may have to operate in the same spectral bands, for example: LTE, 5G, WiFi, Citizens Broadband Radio Service and S-band radars. A comprehensive review of various approaches for solving this problem is presented in [3]. Only a few recent works have focused on analyzing the interference that radar and communications systems cause to each other [4], [5], while many others have proposed a variety of coexistence methods. As pointed out in [3], two main approaches are considered in the literature: addressing only the coexistence problem and considering cooperation between the two systems as well. In the plain coexistence scenario, each system tries to mitigate the interference from the other systems. In a cooperative scenario, there is some exchange of information between the two systems such as channel state or experienced interference levels. In this paper, an interference mask imposed by the communications system is considered to be available at the radar system. Existing system designs in the literature can also be classified in two categories: physically co-located or distinct devices in different locations. In this work, the two systems are considered to be displaced such that the radar system is able to receive also the communications transmissions. From the system architecture point of view, both SISO [6]–[8] and MIMO [9]–[13] configurations are considered in the literature. Both single carrier [6], [14] and multicarrier waveforms [5], [7], [15]–[18] have been employed. Most related papers propose systems in which the radar and the communications waveforms are distinct, while some propose systems where waveforms have dual purpose, i.e. simultaneously carry both payload data and radar signals [9], [19], [20]. Systems that are able to perform both communications and radar tasks, however using different waveforms were proposed in [3], [19], [20]. There is also a trend towards RF convergence where similar waveforms may be used for radar and communications purposes [3]. In this work, SISO radar and communications systems with distinct waveforms are considered.

When considering separate waveforms for radar and communications purposes various optimization strategies have been proposed. Many take radar-centric approaches (aiming at optimizing or adapting only the radar waveform) [3], [6], [11]–[14], [21], [22], whereas communications-centric approaches (aiming at optimizing or adapting only the communications waveform) have been considered in [3], [10], [16], [23]–[25]. A joint design strategy is adopted for example in [3], [26]–[28]. Various criteria have been used for waveform optimization, for example SINR at the radar receiver [6], Mutual Information (MI) [7], [17], or probability of detection [18]. To the author's best knowledge there is no work focused on optimizing the radar waveform for the target parameter estimation performance in cooperative coexistence scenarios.

Novel bounds on estimation performance, from an information-theoretic point of view, were introduced in [29]. The radar and the communications system considered for the joint design in [29] are operating in the same spectral band. Cramér-Rao Bound (CRB) for parameter estimation in a cooperative scenario, where the two systems are in different locations and share the same spectral band, was introduced in [30]. It was shown, using both analytical methods and simulation results, that a radar can improve its estimation performance and have a lower CRB by exploiting the communications signals in a passive way. In this paper, an extended target is

M. Bică and V. Koivunen are with the Department of Signal Processing and Acoustics, School of Electrical Engineering, Aalto University, Konemiehentie 2 FI-02150 Espoo, Finland (e-mail:{firstname.lastname}@aalto.fi).

considered and an estimation-theoretic quantity, namely Fisher Information (FI), is derived for target's time delay estimation. Radar waveform optimization methods are proposed and objective functions that minimize the CRB for target's time delay estimation are derived. When the communications signal is exploited, the additivity property of the FI will lower the CRB compared to the situation where the radar operates alone.

The main contributions of this paper are summarized as follows:

- Estimation-theoretic quantities, namely FI and CRB, are analytically derived for radar-communications cooperation for both known and unknown target channel tap amplitudes.
- Radar waveform optimization based on CRB is proposed and power allocation per subcarrier solutions are provided.
- It is demonstrated, using simulations, that constraining the Subcarrier Power Ratio (SPR) of the transmitted waveform for a more even power distribution over subcarriers can reduce the ambiguities in delay domain.
- The Root Mean Squared Error (RMSE) for the proposed optimized waveforms is evaluated using simulation results and compared with a waveform optimized for received SNR maximization.

This paper is organized as follows. Section II introduces the cooperative model and describes the modeling and the processing of the received signals at the radar receiver. In Section III the estimation bounds for the target's time delay are analytically derived. Radar waveform optimization based on the minimization of the derived bounds (CRB) is presented in Section IV. The ambiguity of the optimized waveforms is analyzed in Section V and a method to reduce it is proposed. In Section VI the target parameter estimation performance of the optimized waveforms is analyzed and compared with the one for a waveform optimized for received SNR maximization. Section VII concludes the paper. In Table I the most common used abbreviations in this paper are provided.

Notations: A lower capital bold letter $\mathbf{x}$ denotes a column vector, while an upper capital bold letter $\mathbf{X}$ denotes a matrix. By $x[l]$ we denote the lth element in a vector $\mathbf{x}$ and by $[\mathbf{X}]_{i,j}$ we denote the ith row and jth column element in a matrix $\mathbf{X}$. The Hermitian transpose of a matrix is denoted by $\mathbf{X}^H$, while the complex conjugate is denoted by $\mathbf{X}^*$. The frequency domain form of a signal is indicated by superscript F. Symbol $\odot$ denotes the element-wise matrix/vector product, symbol $*$ denotes the convolution operation, while $\succeq$ denotes element-wise larger or equal to in case of vectors and matrices. $\mathrm{diag}\{\mathbf{x}\}$ is a diagonal matrix which has the entries of $\mathbf{x}$ on the main diagonal. $\det\{\mathbf{X}\}$ is the determinant of matrix $\mathbf{X}$.

II. Signal Model

In this paper, the multicarrier model introduced in [18] is employed in order to describe the cooperation. A simplified version for one communications base station (BS) is presented in Fig. 1. The radar and communications systems are assumed to be distinct and in different locations. Therefore, the monostatic radar receives echoes off the target due to the transmitted

Table I
List of Abbreviations

	Description
CRB	Cramér-Rao Bound
FI	Fisher Information
OFDM	Orthogonal Frequency Division Multiplexing
RMSE	Root Mean Squared Error
SIC	Successive Interference Cancellation
SPR	Subcarrier Power Ratio

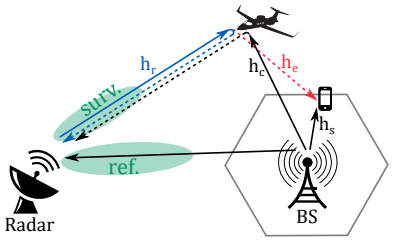

Figure 1. Simplified system model for spectrum sharing between radar and communications system.

and reflected radar signal as well as the communications signals from the BS, whose location is assumed to be known. The communications signal is received via two channels: one which is due to scattering off the target and one corresponding to a direct path. It is assumed that the radar is capable of beamforming in two directions, one required for target surveillance and one for receiving the reference communications signal through the direct path. This can be used to reliably estimate the transmitted communications symbols. Beamforming also rejects interferences from other angles. Consequently, the radar receives the following signals:

$$\begin{aligned} y_{\mathrm{surv}}(t) &= y_{\mathrm{rad}}(t) + y_{\mathrm{com}}(t) + n(t) \\ y_{\mathrm{ref}}(t) &= y_d(t) + n(t), \end{aligned} \tag{1}$$

where $y_{\mathrm{surv}}(t)$ and $y_{\mathrm{ref}}(t)$ are the received signals on the surveillance and reference channels respectively. In addition, $y_{\mathrm{rad}}(t)$ is the radar off the target return, $y_{\mathrm{com}}(t)$ is the communications signal reflected off the target and $y_d(t)$ is the reference communications signal arriving on the direct path, while $n(t)$ accounts for the receiver noise.

In this paper the following assumptions are made:

- The radar is able to beamform in two different directions simultaneously, or has two directional antennas available for the surveillance and reference channels respectively.
- The target is considered static over the observation interval, thus no Doppler effect is considered.
- The transmitted communications symbols are known at the radar or can be reliably estimated from the direct path.
- The same number of L taps for the target impulse response of both the radar and the communications channels is assumed known.
- Both the radar and the communications systems utilize multicarrier waveforms, in particular OFDM with N subcarriers in this paper.

At the radar receiver, on the surveillance direction, the delayed radar signal is superimposed with the delayed commu-

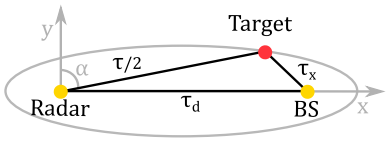

Figure 2. Geometry of the first path of the communications signal reflected off the target and the direct line of sight path. α represents the complement of the angle that the radar surveillance beam is making with the reference beam.

nications signal, both reflected off the target. For an extended target, the equation for the signal at the radar receiver can be written as:

$$\begin{aligned} y_{\text{surv}}(t) &= y_{\text{rad}}(t) + y_{\text{com}}(t) + n(t) \\ &= r(t) * h_r(t) + c(t) * h_c(t) + n(t), \end{aligned} \tag{2}$$

where $r(t)$ and $c(t)$ are the OFDM transmitted radar and communications signals respectively, while $h_r(t)$ and $h_c(t)$ are the radar and the communications channel impulse responses containing the target response. In this paper, an extended target model is considered, similar to [31]. Consequently, the target channel is a periodic channel with L taps spaced at intervals equal to the sampling time T_s [32]. Such target impulse response is modeled for the radar and the communications signal as:

$$h_r(t) = \sum_{l=0}^{L-1} b_{r,l}\delta(t-\tau_{r,l}), \quad h_c(t) = \sum_{l=0}^{L-1} b_{c,l}\delta(t-\tau_{c,l}), \tag{3}$$

respectively. In (3) $b_{r,l}$ and $\tau_{r,l}$ denote the complex amplitude and the time delay for the lth path (tap) in the radar channel, respectively. $b_{c,l}$ and $\tau_{c,l}$ are the communications channel counterparts. The delays $\tau_{r,l}$, with $l = 0 \dots L-1$, are given by:

$$\tau_{r,l} = \tau + lT_s, \tag{4}$$

where τ is the round-trip delay experienced by the radar signal and T_s is the sampling instant. Similarly, for the communications signal:

$$\tau_{c,l} = \tau_c + lT_s, \tag{5}$$

where τ_c is the delay experienced by the communications signal on the first path. As illustrated in Fig. 2 for the first path, the delay experienced by the communications signal is:

$$\tau_c = \tau/2 + \tau_x, \tag{6}$$

where τ_x is the delay from the BS to the target and $\tau/2$ is the one way delay from the target to the radar. It is also illustrated that both the radar and the communications signals experience the same delay $\tau/2$ from the target to the radar, as these travel the same distance.

In the considered cooperative scenario, the goal of the radar is to improve its estimation performance by exploiting the communications signals reflected off the target in a passive manner. The parameter of interest to the radar is the round-trip delay τ, which appears in both signal models for the reflected radar and communications signals in (2). In order to make use of the different observations of the same parameter τ, the received signal on the surveillance direction presented in (2) needs to be separated in two parts: one with the radar component only and one with the communications component, free from mutual interference. One way of achieving the separation is to use the technique of Successive Interference Cancellation (SIC), as presented in [29], [33] for example. This technique involves removing the radar or the communications signal (the strongest one) from the observed signal in order to obtain the communications or the radar return, respectively, free from interference. This approach is applicable if the transmitted communications and radar signals are digital, with the radar symbols drawn from a finite alphabet, for example polyphase P3 and P4 codes. For analog modulated radar and communications signals, source separation techniques, such as blind source separation or independent component analysis (ICA) can be used instead, as long as the signals are statistically independent [34]. In this paper, it is assumed that SIC is used for separating the radar and communications signals since both of them use digital (discrete-time) waveforms. Two cases are considered: the more common case where the radar return is stronger and another one where the communications return is stronger. This impacts the way SIC is implemented, which is discussed in the following Section II-A.

A. SIC Example

In this paper, a crucial assumption made is that the radar and communications signals can be reliably separated. Since both systems are assumed to use digital multicarrier waveforms, SIC methods may be employed. SIC is employed such that the strongest component is first removed from the signal. The SIC technique has been employed in coexisting radar/communications literature, for example [29], [33].

In the following, an example on how SIC could separate the two target returns is provided, in the same spirit as in [29], [33]. Consequently, the radar return is reconstructed based on a predicted round-trip time delay and such reconstructed signal would be removed from the received $y_{\text{surv}}(t)$. The reconstructed radar return is $y_{\text{r,recon}}(t)$ and it is assumed that $y_{\text{rad}}(t) = y_{\text{r,recon}}(t) + e(t)$, where $e(t)$ is a residual error term accounting for the reconstruction error, as in [29]. This prediction error is assumed to be independent of the noise [29]. The separated communications return is obtained as follows:

$$y_{\text{surv}}(t) - y_{\text{r,recon}}(t) = y_{\text{com}}(t) + n(t) + e(t). \tag{7}$$

Consequently, the following set of measurements is obtained:

$$\begin{aligned} y_r(t) &= y_{\text{r,recon}}(t) = y_{\text{rad}}(t) + e(t) \\ y_c(t) &= y_{\text{surv}}(t) - y_{\text{r,recon}}(t) = y_{\text{com}}(t) + n(t) + e(t). \end{aligned} \tag{8}$$

Similarly, when the communications return is stronger this is first removed from the received $y_{\text{surv}}(t)$. Assuming the radar learns the target channel also using only the passive communications reception, it can predict the delay experienced by the communications signal. Using the predicted delay, the communications signal is reconstructed as $y_{\text{c,recon}}(t)$ and it is assumed that $y_{\text{com}}(t) = y_{\text{c,recon}}(t) + e(t)$, with $e(t)$ accounting for the reconstruction error. Thus, the measurements become:

$$\begin{aligned} y_r(t) &= y_{\text{surv}}(t) - y_{\text{c,recon}}(t) = y_{\text{rad}}(t) + n(t) + e(t) \\ y_c(t) &= y_{\text{c,recon}}(t) = y_{\text{com}}(t) + e(t). \end{aligned} \tag{9}$$

The two considered cases, when the radar or the communications return respectively is stronger, impact the structure of the covariance matrix of the measurements. Nevertheless, the derivation of performance bounds on parameter estimation is done in Section III using a general notation and the exact covariance matrix or its inverse are specified in Section III-C.

B. Processing of Radar and Communications Target Returns

Multicarrier waveforms have been shown to bring many advantages to radars [35]–[38] and are used in the majority of modern wireless communications and broadcasting systems. One of the most common multicarrier waveform is the OFDM waveform, which is also chosen for both radar and communications systems in the cooperative scenario. OFDM waveforms have been shown to provide many benefits including frequency diversiy [39], high compression gain [40], as well as robustness and operation in scenarios with low received signal power or high interference levels [39]. It has been shown that OFDM is a promising choice for radar in several works [41]–[43]. There is also a trend towards RF convergence where the same transceiver structures can be used for both communications and radar purposes [3]. Multicarrier models are particularly suitable for that purpose [38]. Consequently, after employing SIC or any other suitable separation technique, the measurements are described by the following two equations:

$$\begin{aligned} y_r(t) &= r(t) * h_r(t) + v_r(t) \\ y_c(t) &= c(t) * h_c(t) + v_c(t), \end{aligned} \tag{10}$$

where $r(t)$ and $c(t)$ are the OFDM transmitted radar and communications signals respectively, $h_r(t)$ and $h_c(t)$ are the radar and the communications channel impulse responses containing the target information, while $v_r(t)$ and $v_c(t)$ are the additive errors associated with the two sets of measurements. As mentioned in Section II-A two cases arise when employing SIC and, consequently, $v_r(t)$ and $v_c(t)$ need to be specified for each case. When the radar target return is stronger we have $v_r(t) = e(t)$ and $v_c(t) = n(t) + e(t)$. When the communications target return is stronger we have $v_r(t) = n(t) + e(t)$ and $v_c(t) = e(t)$. The measurement model can be written in discrete frequency domain as:

$$\begin{aligned} \mathbf{y}_r^F[k] &= \mathbf{r}^F[k] \sum_{l=0}^{L-1} b_{r,l} \exp(-j2\pi k \Delta f(\tau + lT_s)) + \mathbf{v}_r^F[k] \\ \mathbf{y}_c^F[k] &= \mathbf{c}^F[k] \sum_{l=0}^{L-1} b_{c,l} \exp(-j2\pi k \Delta f(\tau/2 + \tau_x + lT_s)) + \\ &\quad \mathbf{v}_c^F[k], \end{aligned} \tag{11}$$

with $k = -N/2 \ldots N/2 - 1$, where

$$\begin{aligned} &\sum_{l=0}^{L-1} b_{r,l} \exp(-j2\pi k \Delta f(\tau + lT_s)) = \mathbf{h}_r^F[k] \\ &\sum_{l=0}^{L-1} b_{c,l} \exp(-j2\pi k \Delta f(\tau/2 + \tau_x + lT_s)) = \mathbf{h}_c^F[k], \end{aligned} \tag{12}$$

are the frequency domain components of target channels for the radar and communications signals respectively.

It was shown in [30], based on [44], that τ_x can be obtained in closed form as:

$$\tau_x = \frac{\tau_c^2 - 2\tau_c \tau_d \sin\alpha - \tau_d^2}{2(\tau_c - \tau_d \sin\alpha)}, \tag{13}$$

where the angle α represents the complement of the angle that the radar surveillance beam is making with the reference beam. This is achieved by assuming the angle α in Fig. 2 is known, as the radar knows where the antenna beams are pointing, and the delay τ_d between the BS and the radar is known (the location of the BS is known exactly in a cooperative scenario). At the same time, the delay τ_c for the first path of the communications signal can be estimated using a correlation based technique between the known, or decoded communications signal received on the direct path, and the one on the surveillance direction.

After the delay τ_x is obtained, the measurements in (11) corresponding to the communications part are multiplied elementwise by $\exp(j2\pi k \Delta f \tau_x)$ in order to compensate for this delay and obtained as:

$$\mathbf{y}_c^{'F}[k] = \mathbf{c}^F[k] \sum_{l=0}^{L-1} b_{c,l} \exp(-j2\pi k \Delta f(\tau/2 + lT_s)) + \mathbf{v}_c^{'F}[k]. \tag{14}$$

Using matrix notation, the model in (11) can be rewritten as:

$$\begin{aligned} \mathbf{y}_r^F &= \mathbf{R}\mathbf{h}_r^F + \mathbf{v}_r^F = \mathbf{R}\mathbf{A}_r\mathbf{b}_r + \mathbf{v}_r^F \\ \mathbf{y}_c^{'F} &= \mathbf{C}\mathbf{h}_c^{'F} + \mathbf{v}_c^{'F} = \mathbf{C}\mathbf{A}_c\mathbf{b}_c + \mathbf{v}_c^{'F}, \end{aligned} \tag{15}$$

where $\mathbf{R} = \mathrm{diag}\{\mathbf{r}^F\}$ and $\mathbf{C} = \mathrm{diag}\{\mathbf{c}^F\}$ are $N \times N$ diagonal matrices containing the transmitted frequency domain radar and communications symbols respectively on the main diagonal. The elements of matrices $\mathbf{A}_r$ and $\mathbf{A}_c$ of size $N \times L$ are given by $[\mathbf{A}_r]_{k,l} = \exp(-j2\pi k \Delta f(\tau + lT_s))$ and $[\mathbf{A}_c]_{k,l} = \exp(-j2\pi k \Delta f(\tau/2 + lT_s))$ respectively, for $k = -N/2, \ldots, N/2 - 1$ and $l = 0, \ldots, L - 1$. Vectors $\mathbf{b}_r$ and $\mathbf{b}_c$ contain the complex amplitudes of the radar and communications channels taps respectively.

III. Parameter Estimation Bounds

Two sets of measurements are obtained in (15), where the frequency domain samples are expressed as function of the transmitted frequency domain symbols and the effect of the extended target on the transmitted signals. These measurements are stacked into a single vector of measurements of size $2N \times 1$ for the radar and communications components respectively:

$$\mathbf{y}^F = \begin{bmatrix} \mathbf{y}_r^F \\ \mathbf{y}_c^{'F} \end{bmatrix}. \tag{16}$$

Two cases can be considered here: a cooperative case, in which the radar performs the estimation using also the communications signal measurements, and the radar-only case, where the radar performs the estimation using only its own measurements. The cooperative case is of main interest in this paper. The radar-only case is provided here for comparison. In both cases, the parameter of interest is τ, the round-trip delay from radar to the target. Furthermore, the amplitudes $\mathbf{b}_r$ and $\mathbf{b}_c$ of the channel taps may be known or unknown and need to be estimated. It is reasonable to assume that in a target

tracking task, the target impulse responses $h_r(t)$ and $h_c(t)$ are either known or can be reliably estimated. This happens when the considered radar is cognitive and is continuously learning about the environment [45]. Consequently, also the amplitudes $\mathbf{b}_r$ and $\mathbf{b}_c$ can be known. Other possible simplifying assumptions are also presented in Section III-C.

A. Unknown Amplitudes $\mathbf{b}_r$ and $\mathbf{b}_c$

The case when the amplitudes $\mathbf{b}_r$ and $\mathbf{b}_c$ need to be estimated is considered first. Thus, the size $(2L+1)\times 1$ vector of parameters to be estimated is $\boldsymbol{\theta} = \begin{bmatrix}\tau & \mathbf{b}_r^T & \mathbf{b}_c^T\end{bmatrix}^T$.

The measurements vector in (16) is assumed to follow a complex Gaussian distribution $\mathbf{y}^F \sim \mathcal{CN}(\mathbf{m}(\boldsymbol{\theta}), \boldsymbol{\Sigma})$, where the mean vector

$$\mathbf{m}(\boldsymbol{\theta}) = \begin{bmatrix}\mathbf{R}\mathbf{A}_r\mathbf{b}_r \\ \mathbf{C}\mathbf{A}_c\mathbf{b}_c\end{bmatrix} \tag{17}$$

is of size $2N \times 1$ and the covariance matrix

$$\boldsymbol{\Sigma} = \begin{bmatrix}\boldsymbol{\Sigma}_{11} & \boldsymbol{\Sigma}_{12} \\ \boldsymbol{\Sigma}_{21} & \boldsymbol{\Sigma}_{22}\end{bmatrix} \tag{18}$$

is of size $2N \times 2N$.

In the following, the CRB on the performance of the estimation of vector parameter $\boldsymbol{\theta}$ is obtained by finding the expression for the Fisher Information (FI) matrix and inverting it. The details of the FI derivation can be found in Appendix A. The FI matrix is a $(2L+1)\times(2L+1)$ size block matrix with the following structure:

$$\mathrm{FI}_{\mathrm{cp}}^{\mathrm{ua}}(\boldsymbol{\theta}) = \begin{bmatrix}J_{11} & \mathbf{J}_{12} & \mathbf{J}_{13} \\ \mathbf{J}_{21} & \mathbf{J}_{22} & \mathbf{J}_{23} \\ \mathbf{J}_{31} & \mathbf{J}_{32} & \mathbf{J}_{33}\end{bmatrix}, \tag{19}$$

where J_{11} is a scalar corresponding to scalar parameter τ, $\mathbf{J}_{12}$ and $\mathbf{J}_{13}$ are $1 \times L$ vectors, corresponding to $L \times 1$ vector parameters $\mathbf{b}_r$ and $\mathbf{b}_c$ respectively. $\mathbf{J}_{21}$ and $\mathbf{J}_{31}$ are the transposes of $\mathbf{J}_{12}$ and $\mathbf{J}_{13}$ respectively and $\mathbf{J}_{22}$, $\mathbf{J}_{23}$, $\mathbf{J}_{32}$ and $\mathbf{J}_{33}$ are matrices of size $L\times L$. The equivalent FI for the delay parameter τ can be obtained using the Schur complement as:

$$\mathrm{FI}_{\mathrm{cp}}^{\mathrm{ua}}(\tau) = J_{11} - \begin{bmatrix}\mathbf{J}_{12} & \mathbf{J}_{13}\end{bmatrix}\begin{bmatrix}\mathbf{J}_{22} & \mathbf{J}_{23} \\ \mathbf{J}_{32} & \mathbf{J}_{33}\end{bmatrix}^{-1}\begin{bmatrix}\mathbf{J}_{21} \\ \mathbf{J}_{31}\end{bmatrix}, \tag{20}$$

from which the CRB for the delay parameter is obtained as $\mathrm{CRB}_{\mathrm{cp}}^{\mathrm{ua}}(\tau) = \mathrm{FI}_{\mathrm{cp}}^{\mathrm{ua}}(\tau)^{-1}$.

B. Known Amplitudes $\mathbf{b}_r$ and $\mathbf{b}_c$

When the amplitudes $\mathbf{b}_r$ and $\mathbf{b}_c$ are assumed known, the only parameter to be estimated is the delay τ. In this case the FI for delay τ is obtained as:

$$\mathrm{FI}_{\mathrm{cp}}^{\mathrm{ka}}(\tau) = J_{11}, \tag{21}$$

and consequently $\mathrm{CRB}_{\mathrm{cp}}^{\mathrm{ka}}(\tau) = J_{11}^{-1}$. Superscript ka stands for known amplitudes.

C. Simplifying Assumptions

In this section few simplifications are provided based on the assumptions on the measurements errors $\mathbf{v}_r^F$ and $\mathbf{v}_c^{'F}$. In particular, the cases where the radar or the communications return respectively is stronger are considered.

1) Stronger radar return: In this more common case, the error in the measurements are $\mathbf{v}_r^F = \mathbf{e}^F$ and $\mathbf{v}_c^{'F} = \mathbf{e}^F + \mathbf{n}^F$ in discrete frequency domain. It is assumed that the reconstruction error is independent of the noise [29]. Similar to [33], the reconstruction error and the noise can be assumed to be random variables following a Gaussian distribution with zero mean and variances σ_e^2 and σ_n^2 respectively. Under such assumptions it can be calculated that $\boldsymbol{\Sigma}_{11} = \boldsymbol{\Sigma}_{12} = \boldsymbol{\Sigma}_{21} = \sigma_e^2\mathbf{I}$ and $\boldsymbol{\Sigma}_{22} = (\sigma_e^2 + \sigma_n^2)\mathbf{I}$ and, using the Schur complement, $\mathbf{V}_{11} = \frac{\sigma_e^2+\sigma_n^2}{\sigma_e^2\sigma_n^2}\mathbf{I}$, $\mathbf{V}_{12} = \mathbf{V}_{21} = -\frac{1}{\sigma_n^2}\mathbf{I}$ and $\mathbf{V}_{22} = \frac{1}{\sigma_n^2}\mathbf{I}$, with $\mathbf{I}$ the identity matrix of size N. Consequently, terms in (43) can be simplified accordingly.

2) Stronger communications return: In this case, the error in the measurements are $\mathbf{v}_c^{'F} = \mathbf{e}^F$ and $\mathbf{v}_r^F = \mathbf{e}^F + \mathbf{n}^F$ in discrete frequency domain. Similarly to the case when the radar return is stronger, it can be calculated that $\boldsymbol{\Sigma}_{11} = (\sigma_e^2 + \sigma_n^2)\mathbf{I}$ and $\boldsymbol{\Sigma}_{12} = \boldsymbol{\Sigma}_{21} = \boldsymbol{\Sigma}_{22} = \sigma_e^2\mathbf{I}$ and, using the Schur complement, $\mathbf{V}_{11} = \frac{1}{\sigma_n^2}\mathbf{I}$, $\mathbf{V}_{12} = \mathbf{V}_{21} = -\frac{1}{\sigma_n^2}\mathbf{I}$ and $\mathbf{V}_{22} = \frac{\sigma_e^2+\sigma_n^2}{\sigma_e^2\sigma_n^2}\mathbf{I}$.

D. Radar-only Case

For comparison with the previous derived CRBs, the case where the radar operates alone is also considered. This corresponds to the case when the radar does not exploit the communications signal. Two CRBs for the radar only case are presented, for the case when the amplitudes $\mathbf{b}_r$ are unknown and known respectively. The radar-only case corresponds to the measurements model in (16) containing only $\mathbf{y}_r^F$.

This measurements vector follows a complex Gaussian distribution $\mathbf{y}^F \sim \mathcal{CN}(\mathbf{m}(\boldsymbol{\theta}), \boldsymbol{\Sigma})$, where the mean $\mathbf{m}(\boldsymbol{\theta}) = \mathbf{R}\mathbf{A}_r\mathbf{b}_r$ is of size $N \times 1$ and the covariance matrix $\boldsymbol{\Sigma}$ is of size $N \times N$.

When the amplitudes $\mathbf{b}_r$ are unknown, the $(L+1)\times 1$ vector of parameters to be estimated is $\boldsymbol{\theta} = \begin{bmatrix}\tau & \mathbf{b}_r^T\end{bmatrix}^T$ and the FI matrix is a $(L+1)\times(L+1)$ size block matrix with the following structure:

$$\mathrm{FI}_{\mathrm{ro}}^{\mathrm{ua}}(\boldsymbol{\theta}) = \begin{bmatrix}J_{11}^{\mathrm{ro}} & \mathbf{J}_{12}^{\mathrm{ro}} \\ \mathbf{J}_{21}^{\mathrm{ro}} & \mathbf{J}_{22}^{\mathrm{ro}}\end{bmatrix}, \tag{22}$$

with each element presented in Appendix B. The equivalent FI for the delay parameter is obtained as:

$$\mathrm{FI}_{\mathrm{ro}}^{\mathrm{ua}}(\tau) = J_{11}^{\mathrm{ro}} - \mathbf{J}_{12}^{\mathrm{ro}}(\mathbf{J}_{22}^{\mathrm{ro}})^{-1}\mathbf{J}_{12}^{\mathrm{ro}T}. \tag{23}$$

Consequently, $\mathrm{CRB}_{\mathrm{ro}}^{\mathrm{ua}}(\tau) = \mathrm{FI}_{\mathrm{ro}}^{\mathrm{ua}}(\tau)^{-1}$. The subscript ro stands for radar-only.

When the amplitudes $\mathbf{b}_r$ are known, the FI for the delay parameter τ is obtained as:

$$\mathrm{FI}_{\mathrm{ro}}^{\mathrm{ka}}(\tau) = J_{11}^{\mathrm{ro}} \tag{24}$$

and consequently $\mathrm{CRB}_{\mathrm{ro}}^{\mathrm{ka}}(\tau) = J_{11}^{\mathrm{ro}-1}$. Similar to the cooperative case, simplifying assumptions can be made. For example, when the noise of the measurement is zero-mean Gaussian with variance $\sigma_{v_r}^2$, the covariance matrix is $\boldsymbol{\Sigma} = \sigma_{v_r}^2\mathbf{I}$ and its inverse $\boldsymbol{\Sigma}^{-1} = \frac{1}{\sigma_{v_r}^2}\mathbf{I}$.

In Fig. 3 it is illustrated a comparison between the CRBs for delay parameter τ in the cooperative and radar-only case,

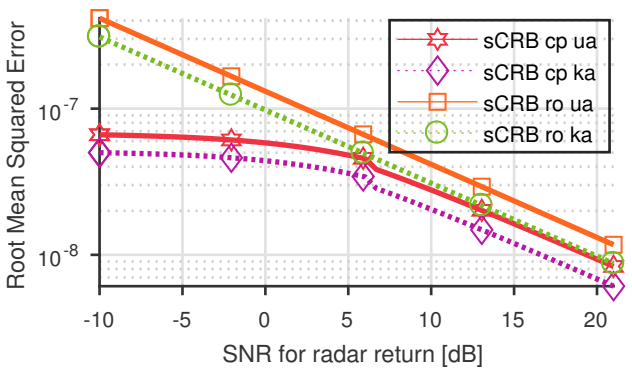

Figure 3. Square root of CRB for the cooperative and the radar-only cases with and without known amplitudes. For the cooperative case it is considered the $\mathrm{SNR}_{\mathrm{com}} = 6$ dB, which is visible on the CRB plots for the cooperative case as the point where SIC removes first the communications and then the radar return and $\mathbf{\Sigma}$ changes. As the CRBs are lower, it is always beneficial to use cooperation and communications signal. Also, when the channel amplitudes are estimated, the estimation performance is degraded compared to the case when the channel amplitudes are known.

as well as known and unknown target channels amplitudes. It can be observed that the CRBs can be grouped in two: one for known and one for unknown target channel amplitudes. Also, the following relations can be established:

$$\mathrm{CRB}^{\mathrm{ua}}_{\mathrm{ro}} \geq \mathrm{CRB}^{\mathrm{ua}}_{\mathrm{cp}} \quad \text{and} \quad \mathrm{CRB}^{\mathrm{ka}}_{\mathrm{ro}} \geq \mathrm{CRB}^{\mathrm{ka}}_{\mathrm{cp}}, \tag{25}$$

together with the observation that the quality of the delay estimates obtained in the cooperative case are theoretically better than the estimates obtained using the radar signal only. The point at 6 dB, when the radar becomes stronger than the communications return and is removed first in the SIC example described in Section II-A is visible on the CRB plots in Fig. 3 due to the change in $\mathbf{\Sigma}$.

IV. Waveform Optimization

The goal is to find the optimum radar waveform that maximizes the FI or minimizes the CRB for estimating target parameters. In this paper the delay parameter τ is considered. The optimization is done by adjusting the transmitted radar power on each subcarrier. The communications signal is not optimized or altered in any way.

The most general form of CRB derived in this paper for the cooperative scenario, when the amplitudes $\mathbf{b}_r$ and $\mathbf{b}_c$ are unknown, is considered for the objective function of the following waveform optimization problems. This corresponds to the FI given in (23), under the assumption that the reconstruction error and the noise are independent and follow a zero mean Gaussian distribution with variances σ_e^2 and σ_n^2 respectively. As mentioned in Section III-C, these assumptions provide some simplifications to the formulations in (43). The objective function to be minimized is $\mathrm{CRB}^{\mathrm{ua}}_{\mathrm{cp}}(\tau) = \mathrm{FI}^{\mathrm{ua}}_{\mathrm{cp}}(\tau)^{-1}$. Consequently, the constrained optimization problem can be stated as follows:

$$\begin{aligned} \underset{\mathbf{r}^F}{\text{minimize}} \quad & \mathrm{CRB}^{\mathrm{ua}}_{\mathrm{cp}} \\ \text{subject to} \quad & (\mathbf{r}^F)^H \mathbf{r}^F \leq P_{\mathrm{T}} \\ & (\mathbf{r}^F)^* \odot \mathbf{r}^F \preceq \mathbf{u}, \end{aligned} \tag{26}$$

where P_{T} is the maximum allowed transmitted radar power and $\mathbf{u}$ is the vector containing the maximum transmitted power on each subcarrier. The latter constraint is due to the desired data rate for the communications users. This desired data rate translates to a minimum SINR and consequently a maximum interference at the communications receiver. In order to limit the radar interference for the communications user a limit on the radar power per subcarrier is needed (which is given by $\mathbf{u}$). An example of how vector $\mathbf{u}$ can be obtained from a minimum data rate for the communications user is presented for example in [17]. In particular, for the assumptions considered in [17], the constraint on the desired rate of each channel for a given data transmission inside the communications system is formulated as:

$$\log\left(1 + \frac{|\mathbf{c}^F[k]|^2 \boldsymbol{\sigma}^2_{h_s}[k]}{|\mathbf{r}^F[k]|^2 \boldsymbol{\sigma}^2_{h_e}[k] + \sigma_n^2}\right) \geq \mathbf{t}[k],$$

where $|\mathbf{r}^F[k]|^2$ and $|\mathbf{c}^F[k]|^2$ are the powers of the radar and the communications signals, respectively, for the kth subcarrier. $\boldsymbol{\sigma}^2_{h_s}[k]$, $\boldsymbol{\sigma}^2_{h_e}[k]$ and σ_n^2 are the gain of the communications channel inside the cell and the gain of the channel on which the radar signal arrives at the communications receiver reflected off the target and the power of the noise at the communications receiver, respectively, for the kth subcarrier. $\mathbf{t}[k]$ is the desired communications rate on kth subcarrier. Clearly the SINR at the communications receiver plays a key role as the desired rate is expressed as $\log(1+\mathrm{SINR})$. Consequently, the communications system senses the interference level and feeds back to the radar a power constraint per subcarrier such that it can maintain a desirable quality of service for its users. The elements of vector $\mathbf{u}$ can be obtained as:

$$\mathbf{u}[k] = \frac{1}{\boldsymbol{\sigma}^2_{h_e}[k]} \left[\frac{|\mathbf{c}^F[k]|^2 \boldsymbol{\sigma}^2_{h_s}[k]}{\exp(\mathbf{t}[k]) - 1} - \sigma_n^2[k] \right]. \tag{27}$$

Even though some simplifications to $\mathrm{CRB}^{\mathrm{ua}}_{\mathrm{cp}}$ are possible, as stated in the beginning of this section, the optimization problem in (26) is non-convex and can not be solved in a closed form. However, a local solution can be provided by solving the problem numerically using the *fmincon* function in Matlab. An interior point algorithm may be used, with the power constraints in (26) introduced as nonlinear constraints. This numerical method does not guarantee a global optimum is obtained. Nevertheless, it is shown that even with this suboptimal solution the radar system can benefit from the cooperation with the communications system by improving its estimation error, namely the RMSE.

It is known that the unconstrained waveform optimization (in particular optimizing power allocation over subcarriers) based on the CRB does not provide practically realizable waveforms [46]–[48]. This is due to the fact that, in a frequency flat channel gain case, CRB is minimized when the Gabor bandwidth (also known as RMS or effective bandwidth) is maximized. For the case of an OFDM waveform and a non-frequency flat channel gain case, the objective to be maximized is of the following form:

$$\frac{1}{\sigma_n^2} \sum_{k=-N/2}^{N/2-1} k^2 |g^F[k]|^2 |r^F[k]|^2, \tag{28}$$

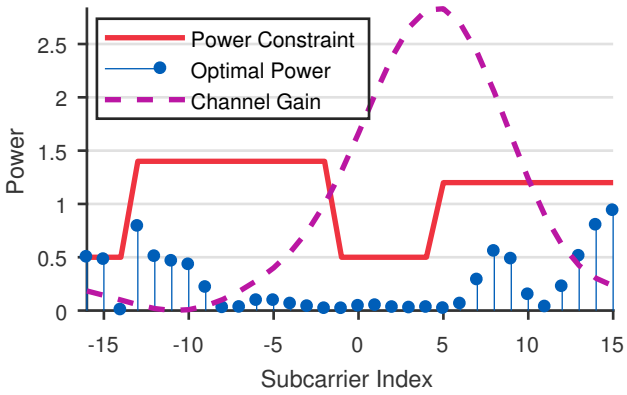

(a) Optimized power allocation example for $P_{\mathrm{T}} = 8$.

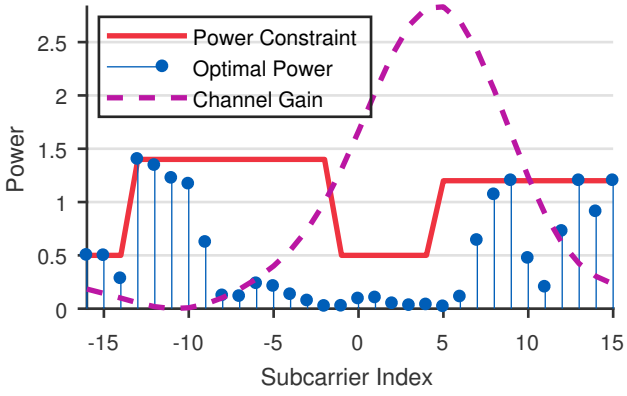

(b) Optimized power allocation example for $P_{\mathrm{T}} = 16$.

Figure 4. Optimized power allocations using fmincon for the cooperative case with unknown channel amplitudes. The trade-off between allocating power based on channel gain or subcarrier index is observed.

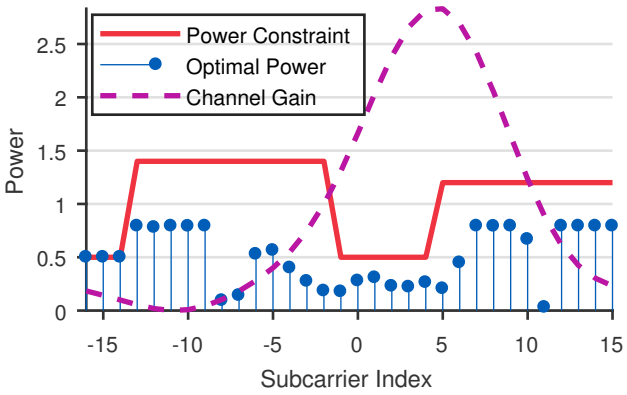

(a) Optimization using SPR = 2 dB.

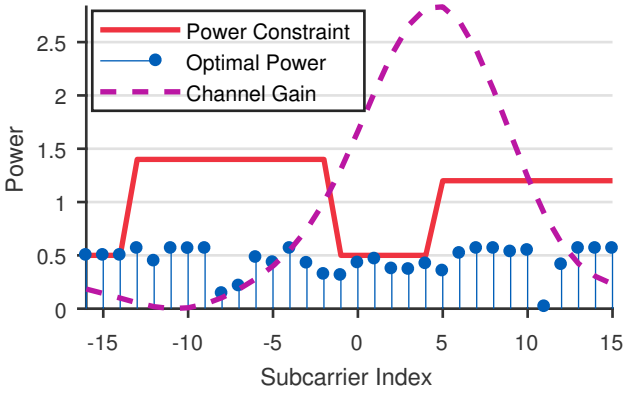

(b) Optimization using SPR = 1 dB.

Figure 5. Optimized power allocations using fmincon Subcarrier Power Ratio (SPR) constraint. For all optimizations the total power constraint $P_{\mathrm{T}} = 16$. As expected, the SPR constraint forces a more uniform power allocation over subcarriers.

where k is the subcarrier index, $|g^F[k]|^2$ is the channel gain on the kth subcarrier and the maximization is done with respect to the radar power on the kth subcarrier $|r^F[k]|^2$. It is observed from (28) that power is allocated to subcarrier which have a larger combination of gain and index. Although the objective of (26) is more complex than the one in (28), its main terms follow the form of (28). Consequently, (28) provides a good example for how power is allocated in (26). Nevertheless, when maximizing the objective in (26) the subcarrier index is emphasized more than the subcarrier gain in the optimization. Consequently, for a waveform optimized using the formulation in (26) there will be a trade-off between power allocation to the subcarriers on the edge of the spectrum and to the subcarriers where the channel gain is stronger and communications rate constraint is less strict. This is observed in Fig. 4 for two constraints on the total transmitted radar power. The trade-off is better visible when the total transmitted radar power is smaller, as power allocation is more important in a more strictly power-constrained regime rather than power-unconstrained regime (for example the radar can transmit all the time at maximum power).

For the waveform optimization simulations in this paper waveforms with $N = 32$ subcarriers and intercarrier spacing $\Delta f = 200$ kHz are considered. Both the radar and communications target channels are considered to have $L = 4$ taps. The tap amplitudes are arbitrarily selected as: $\mathbf{b}_r = [0.38 + 0.23i \;\; 1.1 - 0.92i \;\; -1.5 - 0.31i \;\; 0.61 + 0.24i]^T$ and $\mathbf{b}_c = [1.38{+}0.63i \;\; 1.1{-}0.62i \;\; -1.6{-}0.91i \;\; 0.81{+}0.14i]^T$. For the communications return it is considered that $\mathrm{SNR}_{\mathrm{com}} = 6$ dB. The total radar power constraint P_{T} is chosen as either 8 or 16.

V. Ambiguity of the Optimized Waveforms

It is of importance to consider the ambiguity functions of the optimized waveforms. Waveform optimization based on CRB results in waveforms with high ambiguity. It is demonstrated that by constraining the Subcarrier Power Ratio (SPR), which is a measure of how much the maximum power of a certain subcarrier deviates from the average subcarrier power, the delay domain ambiguity can be reduced. The SPR constraint distributes the available power more evenly in the available spectrum. This reduces time domain correlations of the signal, as it directly impacts the shape of the signal. In contrast to the Peak to Average Power Ratio (PAPR), the SPR is computed in frequency domain. The SPR is defined as:

$$\mathrm{SPR} = \frac{\max_k |\mathbf{r}^F[k]|^2}{\frac{1}{N}\|\mathbf{r}^F\|^2}, \tag{29}$$

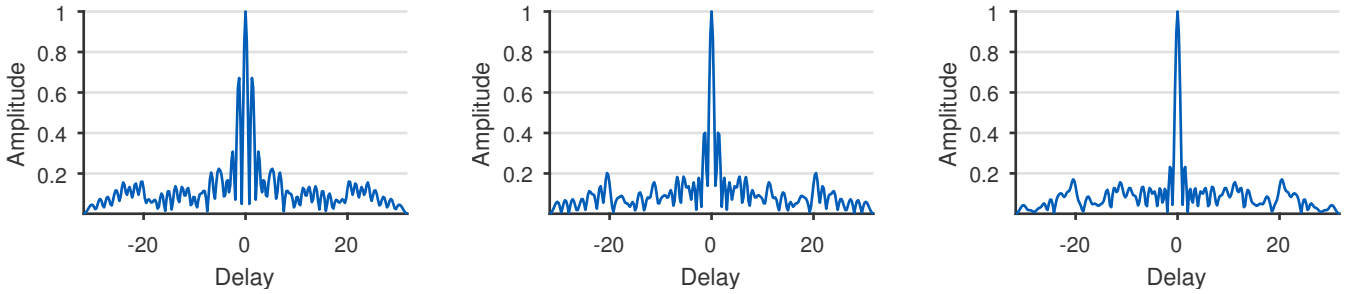

(a) $P_{\mathrm{T}} = 16$, no SPR constraint. (b) $P_{\mathrm{T}} = 16$, SPR = 2 dB. (c) $P_{\mathrm{T}} = 16$, SPR = 1 dB.

Figure 6. Autocorrelation function for different SPR constraints. It is observed that the SPR constraint can decrease the ambiguities in the delay domain.

where N is the number of subcarriers. Consequently, for a maximum allowed SPR, the power on kth subcarrier needs to satisfy the following condition:

$$|\mathbf{r}^F[k]|^2 \leq \frac{1}{N}\|\mathbf{r}^F\|^2 \mathrm{SPR}_{\max}, \tag{30}$$

where $\mathrm{SPR}_{\max}$ is the maximum allowed SPR. Thus, the optimization problem incorporating this constraint is:

$$\begin{aligned} \underset{\mathbf{r}^F}{\text{minimize}} \quad & \mathrm{CRB}_{\mathrm{cp}}^{\mathrm{ua}} \\ \text{subject to} \quad & (\mathbf{r}^F)^H \mathbf{r}^F \leq P_{\mathrm{T}} \\ & (\mathbf{r}^F)^* \odot \mathbf{r}^F \preceq \mathbf{u} \\ & (\mathbf{r}^F)^* \odot \mathbf{r}^F \preceq \tfrac{1}{N}\|\mathbf{r}^F\|^2 \mathrm{SPR}_{\max}. \end{aligned} \tag{31}$$

Similar to the optimization problem in (26), this problem can be solved numerically using *fmincon* in Matlab.

In Fig. 5 a comparison between optimized power allocations using different SPR constraints of 1 dB and 2 dB is presented. It is observed that, as expected, the SPR constraint forces a more uniform power allocation over the subcarriers in comparison to the optimized power allocation presented in Fig. 4b.

The ideal ambiguity function has a thumbtack shape. The delay domain ambiguity of optimized radar waveforms is compared by analyzing the autocorrelation function plots for these waveforms. In Fig. 6 the autocorrelation plots for the waveforms optimized using SPR constraints are shown in comparison with the one optimized without the SPR constraint. All waveforms considered for Fig. 6 are optimized for a maximum total transmitted power of $P_{\mathrm{T}} = 16$ and the same set of randomly chosen N phases between 0 and 2π for each subcarrier is considered for the autocorrelation plots.

VI. Estimation Performance

The goal for the waveform optimization proposed in this paper is to obtain a waveform that improves the time delay estimation. The estimation error, obtained using the optimized waveforms in Section V for the case of unknown channel amplitudes and an SPR constraint of 1 dB, is evaluated and compared with the one achieved by a waveform optimized for maximizing the received SNR. It is shown that the estimation error of the latter is larger than the error for the optimized waveforms proposed in this paper. Also, the estimation error for the cooperative and radar-only cases is compared and the benefit of exploiting the communications signal in a passive manner is shown. The RMSE is used to compare the estimation errors. A single radar channel realization is used in the simulations as an illustrative example on how channel quality plays a role in optimization, however extensive simulations for many different channel realizations have not been studied.

The joint density of the measurements in (16), given the assumptions in this paper, is:

$$f(\mathbf{y};\boldsymbol{\theta}) = \frac{1}{\pi \det(\boldsymbol{\Sigma})} \exp\left(-(\mathbf{y}-\mathbf{m})^H \boldsymbol{\Sigma}^{-1}(\mathbf{y}-\mathbf{m})\right), \tag{32}$$

where $\det(\boldsymbol{\Sigma})$ is the determinant of $\boldsymbol{\Sigma}$ and the corresponding log likelihood function is:

$$l(\mathbf{y};\boldsymbol{\theta}) = -\ln(\pi \det(\boldsymbol{\Sigma})) - (\mathbf{y}-\mathbf{m})^H \boldsymbol{\Sigma}^{-1}(\mathbf{y}-\mathbf{m}). \tag{33}$$

The maximum likelihood estimate (MLE) for τ can be obtained as:

$$\hat{\tau}_{ML} = \arg\max_{\tau} l(\mathbf{y};\tau), \tag{34}$$

assuming that the amplitudes are already estimated or assumed known. The negative of the log likelihood function, after ignoring the terms that do not depend on τ, can be written as:

$$\begin{aligned} L(\mathbf{y};\tau) = {} & (\mathbf{y}_r - \mathbf{m}_r(\tau))^H \mathbf{V}_{11}(\mathbf{y}_r - \mathbf{m}_r(\tau)) + \\ & 2\Re\{(\mathbf{y}_r - \mathbf{m}_r(\tau))^H \mathbf{V}_{12}(\mathbf{y}_c - \mathbf{m}_c(\tau))\} + \\ & (\mathbf{y}_c - \mathbf{m}_c(\tau))^H \mathbf{V}_{22}(\mathbf{y}_c - \mathbf{m}_c(\tau)), \end{aligned} \tag{35}$$

where $\mathbf{m}_r(\tau) = \mathbf{R}\mathbf{A}_r(\tau)\mathbf{b}_r$ and $\mathbf{m}_c(\tau) = \mathbf{C}\mathbf{A}_c(\tau)\mathbf{b}_c$. Consequently, the estimate of the time delay is obtained as:

$$\hat{\tau} = \arg\min_{\tau} L(\mathbf{y};\tau). \tag{36}$$

Finding the exact time delay estimate in (36) is not trivial, thus a grid search if performed to obtain $\hat{\tau}$ from its discrete-time model $\tau_m = m\frac{1}{M\Delta f}$, $m = 1 \ldots M$.

For the estimation performance simulations performed in this paper, a number of $M = 96$ discrete bins are chosen for the discretized delay τ_m and number of 10000 noise realizations are considered. The simulation results are presented in Fig. 7 and Fig. 8. In Fig. 7 the strength of the communications return is kept constant for $\mathrm{SNR}_{\mathrm{com}} = 6$ dB. As SIC is employed such that it removes the strongest component first, in Fig. 7a the communications return is removed first, while in Fig. 7b the radar return is removed first. As mentioned in Section II-A, the covariance matrix of the measurements is not the same in both cases, thus the choice to present the

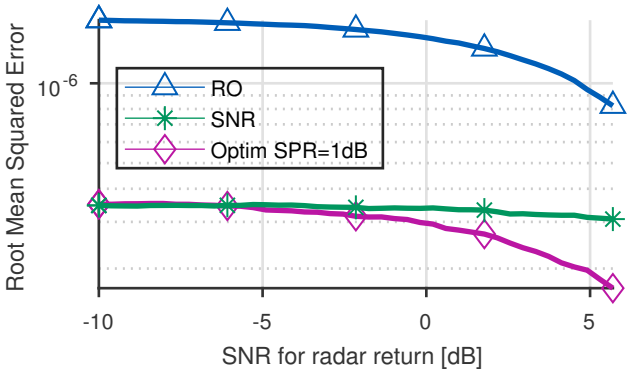

(a) RMSE for $\mathrm{SNR}_{\mathrm{rad}} < \mathrm{SNR}_{\mathrm{com}} = 6$ dB.

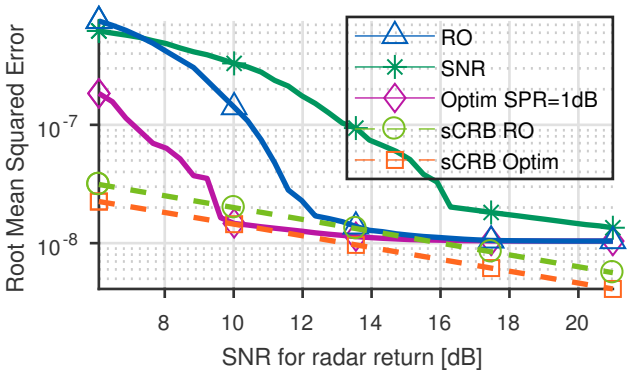

(b) RMSE for $\mathrm{SNR}_{\mathrm{rad}} > \mathrm{SNR}_{\mathrm{com}} = 6$ dB.

Figure 7. RMSE of the waveforms optimized in the case of unknown channel amplitudes with an SPR constraint (1 dB). It is observed that the optimization improves the estimation performance in both low and high SNR regime for the radar return. The limitation of the implemented estimator is also shown in the high SNR regime, where the RMSE becomes flat.

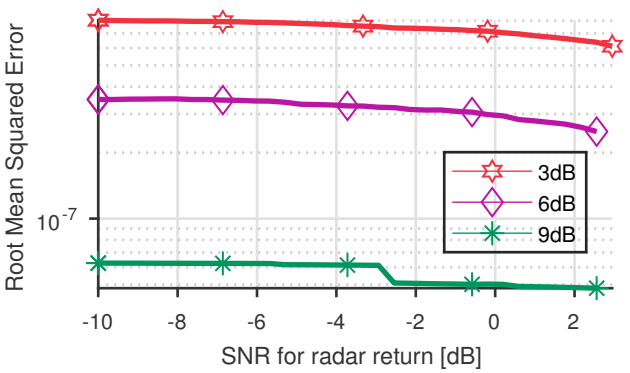

(a) RMSE for $\mathrm{SNR}_{\mathrm{rad}} < \mathrm{SNR}_{\mathrm{com}} = 3$ dB.

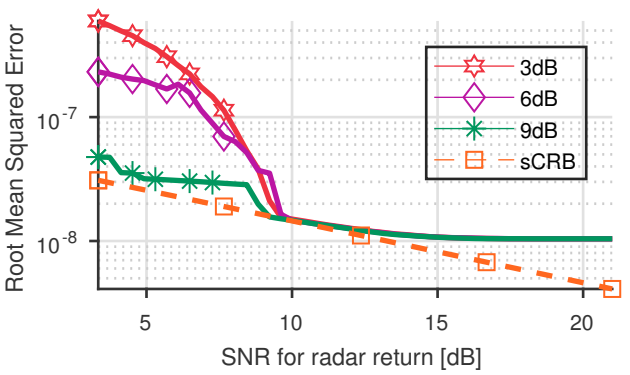

(b) RMSE for $\mathrm{SNR}_{\mathrm{rad}} > \mathrm{SNR}_{\mathrm{com}} = 3$ dB.

Figure 8. RMSE of the waveforms optimized in the case of unknown channel amplitudes with an SPR constraint (1 dB) for different strengths for the communications return. It is observed that the stronger the communications return, the greater the improvement in estimation performance, especially in the low SNR regime for the radar return.

results in two different figures, rather then one figure as it is commonly done in traditional radar literature. In both Fig. 7a and Fig. 7b it is observed that the estimation performance is improved in the cooperative case versus the radar-only case. Also, the waveform optimization based on the CRB provides a waveform with improved estimation performance versus a waveform optimized to maximize the receiver SNR. As the time delay estimator implemented for the performed simulations is based on a grid search, the impact of the grid resolution on the RMSE performance is observed in Fig. 7b. In the high SNR regime the RMSE hits an error floor and does not decrease anymore. In this paper the focus is in emphasizing the benefit of the proposed waveform optimization and the exploitation of the communications signal in a passive manner, thus the performance of the actual estimator is not of concern. In Fig. 8 it is shown the improvement in estimation performance as the strength of the communications return is increased. Again, the limitation of the implemented estimator is observed in Fig. 8 as well.

VII. Conclusions

This paper addresses the problem of waveform optimization for target parameter estimation task in a cooperative scenario between radar and communications systems positioned in different locations. The radar model is cognitive in a sense that it takes into account the target channel gains in the optimization. Fisher Information (FI) and Cramér-Rao Bound (CRB) are analytically derived and radar waveform optimization based on FI and CRB is proposed. The RMSE of the time delay estimation using the optimized radar waveforms is provided in simulation results and compared with the RMSE of a waveform optimized such that the receiver SNR is maximized.

This work shows that the radar waveform can be optimized with the objective of maximizing FI or minimizing CRB in a cooperative scenario with communications systems. Although the objective function is non-convex, a local solution can be provided using numerical optimization. The optimization solutions reveal the trade-off between power allocation based on the channel gain and maximizing the Gabor bandwidth. The latter forces the energy to be allocated at the edges of the spectrum.

Finally, it is demonstrated that, using an additional constraint on the SPR, the power is distributed more evenly over subcarriers and at the same time the ambiguities in the delay domain are reduced. It is also demonstrated that CRB-based radar waveform optimization and exploiting the communications signal in a passive way can improve the estimation performance.

APPENDIX A

Details of the FI derivations for the cooperative case with unknown amplitudes $\mathbf{b}_r$ and $\mathbf{b}_c$ are provided in the following. For the considered case, the general FI expression for the complex Gaussian density function presented in [49] can be used, where each element in the FI matrix is obtained as:

$$[\mathrm{FI}(\boldsymbol{\theta})]_{p,q} = 2\Re\left\{\frac{\partial \mathbf{m}^H(\boldsymbol{\theta})}{\partial \boldsymbol{\theta}_p}\boldsymbol{\Sigma}^{-1}\frac{\partial \mathbf{m}(\boldsymbol{\theta})}{\partial \boldsymbol{\theta}_q}\right\}, \tag{37}$$

where $\boldsymbol{\theta}_p$ and $\boldsymbol{\theta}_q$ are the pth and qth elements in parameter vector $\boldsymbol{\theta}$, with $p, q = 1, \ldots, 2L+1$ and L the number of channel taps. As mentioned already in Section III-A, the FI matrix is a $(2L+1)\times(2L+1)$ size block matrix with the following structure:

$$\mathrm{FI}^{\mathrm{ua}}_{\mathrm{cp}}(\boldsymbol{\theta}) = \begin{bmatrix} J_{11} & \mathbf{J}_{12} & \mathbf{J}_{13} \\ \mathbf{J}_{21} & \mathbf{J}_{22} & \mathbf{J}_{23} \\ \mathbf{J}_{31} & \mathbf{J}_{32} & \mathbf{J}_{33} \end{bmatrix}. \tag{38}$$

It is observed from (37) FI can be computed in blocks for different parameters. Thus, the vector of parameters $\boldsymbol{\theta} = \begin{bmatrix}\tau & \mathbf{b}_r^T & \mathbf{b}_c^T\end{bmatrix}^T$ can be split in τ and $\mathbf{b} = \begin{bmatrix}\mathbf{b}_r^T & \mathbf{b}_c^T\end{bmatrix}^T$ and it can be obtained that:

$$\frac{\partial \mathbf{m}(\boldsymbol{\theta})}{\partial \tau} = \frac{\partial}{\partial \tau}\begin{bmatrix}\mathbf{R}\mathbf{A}_r\mathbf{b}_r \\ \mathbf{C}\mathbf{A}_c\mathbf{b}_c\end{bmatrix} = \begin{bmatrix}(-j2\pi\Delta f)\mathbf{R}\mathbf{A}_r\mathbf{b}_r \\ (-j\pi\Delta f)\mathbf{C}\mathbf{A}_c\mathbf{b}_c\end{bmatrix}, \tag{39}$$

of size $2N\times 1$, and

$$\frac{\partial \mathbf{m}(\boldsymbol{\theta})}{\partial \mathbf{b}} = \frac{\partial}{\partial \mathbf{b}}\begin{bmatrix}\mathbf{R}\mathbf{A}_r\mathbf{b}_r \\ \mathbf{C}\mathbf{A}_c\mathbf{b}_c\end{bmatrix} = \begin{bmatrix}\mathbf{R}\mathbf{A}_r & \mathbf{0} \\ \mathbf{0} & \mathbf{C}\mathbf{A}_c\end{bmatrix}, \tag{40}$$

of size $2N\times 2L$, with $\mathbf{0}$ the size $N\times N$ matrix with all elements 0. The different blocks of the FI matrix in (38) can then be obtained as follows:

$$J_{11} = 2\Re\left\{\left(\frac{\partial \mathbf{m}(\boldsymbol{\theta})}{\partial \tau}\right)^H\boldsymbol{\Sigma}^{-1}\frac{\partial \mathbf{m}(\boldsymbol{\theta})}{\partial \tau}\right\} \tag{41a}$$

$$\begin{bmatrix}\mathbf{J}_{12} & \mathbf{J}_{13}\end{bmatrix} = 2\Re\left\{\left(\frac{\partial \mathbf{m}(\boldsymbol{\theta})}{\partial \tau}\right)^H\boldsymbol{\Sigma}^{-1}\frac{\partial \mathbf{m}(\boldsymbol{\theta})}{\partial \mathbf{b}}\right\} \tag{41b}$$

$$\begin{bmatrix}\mathbf{J}_{21} \\ \mathbf{J}_{31}\end{bmatrix} = 2\Re\left\{\left(\frac{\partial \mathbf{m}(\boldsymbol{\theta})}{\partial \mathbf{b}}\right)^H\boldsymbol{\Sigma}^{-1}\frac{\partial \mathbf{m}(\boldsymbol{\theta})}{\partial \tau}\right\} \tag{41c}$$

$$\begin{bmatrix}\mathbf{J}_{22} & \mathbf{J}_{23} \\ \mathbf{J}_{32} & \mathbf{J}_{33}\end{bmatrix} = 2\Re\left\{\left(\frac{\partial \mathbf{m}(\boldsymbol{\theta})}{\partial \mathbf{b}}\right)^H\boldsymbol{\Sigma}^{-1}\frac{\partial \mathbf{m}(\boldsymbol{\theta})}{\partial \mathbf{b}}\right\}, \tag{41d}$$

each of size 1×1, $1\times 2L$, $2L\times 1$ and $2L\times 2L$ respectively. Applying the results in (39) and (40) to (41) and using the notation

$$\boldsymbol{\Sigma}^{-1} = \begin{bmatrix}\mathbf{V}_{11} & \mathbf{V}_{12} \\ \mathbf{V}_{21} & \mathbf{V}_{22}\end{bmatrix}, \tag{42}$$

were each block is of size $N\times N$, the block elements of the FI matrix are obtained as follows:

$$\begin{aligned} J_{11} = 2\Re\Big\{&(2\pi\Delta f)^2\mathbf{b}_r^H\mathbf{A}_r^H\mathbf{D}\mathbf{R}^H\Big(\mathbf{V}_{11}\mathbf{R}\mathbf{D}\mathbf{A}_r\mathbf{b}_r + \\ &\frac{1}{2}\mathbf{V}_{12}\mathbf{C}\mathbf{D}\mathbf{A}_c\mathbf{b}_c\Big) + \\ &2(\pi\Delta f)^2\mathbf{b}_c^H\mathbf{A}_c^H\mathbf{D}\mathbf{C}^H\Big(\mathbf{V}_{21}\mathbf{R}\mathbf{D}\mathbf{A}_r\mathbf{b}_r + \\ &\frac{1}{2}\mathbf{V}_{22}\mathbf{C}\mathbf{D}\mathbf{A}_c\mathbf{b}_c\Big)\Big\} \end{aligned} \tag{43a}$$

$$\begin{aligned} \mathbf{J}_{12} = 2\Re\Big\{&j2\pi\Delta f\Big(\mathbf{b}_r^H\mathbf{A}_r^H\mathbf{D}\mathbf{R}^H\mathbf{V}_{11}\mathbf{R}\mathbf{A}_r + \\ &\frac{1}{2}\mathbf{b}_c^H\mathbf{A}_c^H\mathbf{D}\mathbf{C}^H\mathbf{V}_{21}\mathbf{R}\mathbf{A}_r\Big)\Big\} \end{aligned} \tag{43b}$$

$$\begin{aligned} \mathbf{J}_{13} = 2\Re\Big\{&j2\pi\Delta f\Big(\mathbf{b}_r^H\mathbf{A}_r^H\mathbf{D}\mathbf{R}^H\mathbf{V}_{12}\mathbf{C}\mathbf{A}_c + \\ &\frac{1}{2}\mathbf{b}_c^H\mathbf{A}_c^H\mathbf{D}\mathbf{C}^H\mathbf{V}_{22}\mathbf{C}\mathbf{A}_c\Big)\Big\} \end{aligned} \tag{43c}$$

$$\mathbf{J}_{22} = 2\Re\left\{\mathbf{A}_r^H\mathbf{R}^H\mathbf{V}_{11}\mathbf{R}\mathbf{A}_r\right\} \tag{43d}$$

$$\mathbf{J}_{23} = 2\Re\left\{\mathbf{A}_r^H\mathbf{R}^H\mathbf{V}_{12}\mathbf{C}\mathbf{A}_c\right\} \tag{43e}$$

$$\mathbf{J}_{32} = 2\Re\left\{\mathbf{A}_c^H\mathbf{C}^H\mathbf{V}_{21}\mathbf{R}\mathbf{A}_r\right\} \tag{43f}$$

$$\mathbf{J}_{33} = 2\Re\left\{\mathbf{A}_c^H\mathbf{C}^H\mathbf{V}_{22}\mathbf{C}\mathbf{A}_c\right\} \tag{43g}$$

$$\mathbf{J}_{21} = \mathbf{J}_{12}^T \tag{43h}$$

$$\mathbf{J}_{31} = \mathbf{J}_{13}^T, \tag{43i}$$

where $\mathbf{D} = \mathrm{diag}\{-N/2, \ldots, N/2-1\}$.

APPENDIX B

For the radar-only case with unknown amplitudes $\mathbf{b}_r$ similar derivations are employed as for the cooperative case with unknown amplitudes presented in Appendix A. The terms corresponding to the communications channel amplitudes $\mathbf{b}_c$ are now eliminated from both $\boldsymbol{\theta}$ and the FI matrix. As mentioned already in Section III-D, in this case the FI matrix is a $(L+1)\times(L+1)$ size block matrix with the following structure:

$$\mathrm{FI}^{\mathrm{ua}}_{\mathrm{ro}}(\boldsymbol{\theta}) = \begin{bmatrix} J_{11}^{\mathrm{ro}} & \mathbf{J}_{12}^{\mathrm{ro}} \\ \mathbf{J}_{21}^{\mathrm{ro}} & \mathbf{J}_{22}^{\mathrm{ro}}\end{bmatrix}. \tag{44}$$

Applying the same procedure as in Appendix A, the block elements of the FI matrix are obtained as follows:

$$J_{11}^{\mathrm{ro}} = 2\Re\left\{(2\pi\Delta f)^2\mathbf{b}_r^H\mathbf{A}_r^H\mathbf{D}\mathbf{R}^H\boldsymbol{\Sigma}^{-1}\mathbf{R}\mathbf{D}\mathbf{A}_r\mathbf{b}_r\right\} \tag{45a}$$

$$\mathbf{J}_{12}^{\mathrm{ro}} = 2\Re\left\{j2\pi\Delta f\mathbf{b}_r^H\mathbf{A}_r^H\mathbf{D}\mathbf{R}^H\boldsymbol{\Sigma}^{-1}\mathbf{R}\mathbf{A}_r\right\} \tag{45b}$$

$$\mathbf{J}_{22}^{\mathrm{ro}} = 2\Re\left\{\mathbf{A}_r^H\mathbf{R}^H\boldsymbol{\Sigma}^{-1}\mathbf{R}\mathbf{A}_r\right\} \tag{45c}$$

$$\mathbf{J}_{21}^{\mathrm{ro}} = \mathbf{J}_{12}^{\mathrm{ro}T}, \tag{45d}$$

where $\mathbf{D} = \mathrm{diag}\{-N/2, \ldots, N/2-1\}$.

ACKNOWLEDGMENT

The authors would like to thank Dr. Hassan Naseri for numerous helpful discussions in developing this work.

REFERENCES

[1] President's Council of Advisors on Science and Technology, "Realizing the Full Potential of Government-Held Spectrum to Spur Economic Growth," July 2012. [Online]. Available: https://obamawhitehouse.archives.gov/sites/default/files/microsites/ostp/pcast_spectrum_report_final_july_20_2012.pdf

[2] Federal Communications Commission (FCC), "FCC Proposes to Enable Innovative Small Cell Use of Spectrum in the 3.5 GHz Band," December 2012. [Online]. Available: https://www.fcc.gov/document/fcc-proposes-innovative-small-cell-use-35-ghz-band

[3] B. Paul, A. R. Chiriyath, and D. W. Bliss, "Survey of RF Communications and Sensing Convergence Research," *IEEE Access*, vol. 5, pp. 252–270, December 2017.

[4] S. Heuel, D. McCarthy, and Y. Shavit, "Test and measurement of coexistence between S-Band radar and mobile networks," in *2016 26th International Conference Radioelektronika (RADIOELEKTRONIKA)*, April 2016, pp. 1–4.

[5] N. Nartasilpa, D. Tuninetti, N. Devroye, and D. Erricolo, "Let's share CommRad: Effect of radar interference on an uncoded data communication system," in *2016 IEEE Radar Conference (RadarConf)*, May 2016, pp. 1–5.

[6] A. Aubry, A. D. Maio, Y. Huang, M. Piezzo, and A. Farina, "A new radar waveform design algorithm with improved feasibility for spectral coexistence," *IEEE Transactions on Aerospace and Electronic Systems*, vol. 51, no. 2, pp. 1029–1038, April 2015.

[7] K. W. Huang, M. Bica, U. Mitra, and V. Koivunen, "Radar Waveform Design in Spectrum Sharing Environment: Coexistence and Cognition," in *2015 IEEE Radar Conference (RadarCon)*, May 2015, pp. 1698–1703.

[8] C. Sahin, J. Jakabosky, P. M. McCormick, J. G. Metcalf, and S. D. Blunt, "A novel approach for embedding communication symbols into physical radar waveforms," in *2017 IEEE Radar Conference (RadarConf)*, May 2017, pp. 1498–1503.

[9] A. Hassanien, M. G. Amin, Y. D. Zhang, and B. Himed, "A dual-function MIMO radar-communications system using PSK modulation," in *2016 24th European Signal Processing Conference (EUSIPCO)*, August 2016, pp. 1613–1617.

[10] E. H. G. Yousif, M. C. Filippou, F. Khan, T. Ratnarajah, and M. Sellathurai, "A new LSA-based approach for spectral coexistence of MIMO radar and wireless communications systems," in *2016 IEEE International Conference on Communications (ICC)*, May 2016, pp. 1–6.

[11] A. Khawar, A. Abdelhadi, and T. C. Clancy, "Coexistence Analysis Between Radar and Cellular System in LoS Channel," *IEEE Antennas and Wireless Propagation Letters*, vol. 15, pp. 972–975, October 2016.

[12] S. Sodagari, A. Khawar, T. C. Clancy, and R. McGwier, "A projection based approach for radar and telecommunication systems coexistence," in *2012 IEEE Global Communications Conference (GLOBECOM)*, December 2012, pp. 5010–5014.

[13] A. Khawar, A. Abdel-Hadi, and T. Clancy, "MIMO radar waveform design for coexistence with cellular systems," in *2014 IEEE International Symposium on Dynamic Spectrum Access Networks (DYSPAN)*, April 2014, pp. 20–26.

[14] A. Aubry, V. Carotenuto, A. D. Maio, A. Farina, and L. Pallotta, "Optimization theory-based radar waveform design for spectrally dense environments," *IEEE Aerospace and Electronic Systems Magazine*, vol. 31, no. 12, pp. 14–25, December 2016.

[15] S. Kim, J. Choi, and C. B. Dietrich, "Coexistence between OFDM and pulsed radars in the 3.5 GHz band with imperfect sensing," in *2016 IEEE Wireless Communications and Networking Conference*, April 2016, pp. 1–6.

[16] S. Kim, J. M. J. Park, and K. Bian, "PSUN: An OFDM scheme for coexistence with pulsed radar," in *2015 International Conference on Computing, Networking and Communications (ICNC)*, February 2015, pp. 984–988.

[17] M. Bica, K. W. Huang, V. Koivunen, and U. Mitra, "Mutual information based radar waveform design for joint radar and cellular communication systems," in *2016 IEEE International Conference on Acoustics, Speech and Signal Processing (ICASSP)*, March 2016, pp. 3671–3675.

[18] M. Bica, K. W. Huang, U. Mitra, and V. Koivunen, "Opportunistic Radar Waveform Design in Joint Radar and Cellular Communication Systems," in *2015 IEEE Global Communications Conference (GLOBECOM)*, December 2015, pp. 1–7.

[19] S. Melo, S. Pinna, A. Bogoni, I. F. da Costa, D. H. Spadoti, F. Laghezza, F. Scotti, and S. A. Cerqueira, "Dual-use system combining simultaneous active radar communication, based on a single photonics-assisted transceiver," in *2016 17th International Radar Symposium (IRS)*, May 2016, pp. 1–4.

[20] A. K. Mishra and M. Inggs, "White space symbiotic radar: A new scheme for coexistence of radio communications and radar," in *2015 IEEE Radar Conference*, October 2015, pp. 56–60.

[21] J. A. Mahal, A. Khawar, A. Abdelhadi, and T. C. Clancy, "Spectral Coexistence of MIMO Radar and MIMO Cellular System," *IEEE Transactions on Aerospace and Electronic Systems*, vol. 53, no. 2, pp. 655–668, April 2017.

[22] M. A. Govoni, "Enhancing spectrum coexistence using radar waveform diversity," in *2016 IEEE Radar Conference (RadarConf)*, May 2016, pp. 1–5.

[23] S. S. Raymond, A. Abubakari, and H. S. Jo, "Coexistence of Power-Controlled Cellular Networks With Rotating Radar," *IEEE Journal on Selected Areas in Communications*, vol. 34, no. 10, pp. 2605–2616, October 2016.

[24] E. Yousif, F. Khan, T. Ratnarajah, and M. Sellathurai, "On the spectral coexistence of colocated MIMO radars and wireless communications systems," in *2016 IEEE 17th International Workshop on Signal Processing Advances in Wireless Communications (SPAWC)*, July 2016, pp. 1–5.

[25] C. Shahriar, A. Abdelhadi, and T. C. Clancy, "Overlapped-MIMO radar waveform design for coexistence with communication systems," in *2015 IEEE Wireless Communications and Networking Conference (WCNC)*, March 2015, pp. 223–228.

[26] B. Li and A. Petropulu, "MIMO radar and communication spectrum sharing with clutter mitigation," in *2016 IEEE Radar Conference (RadarConf)*, May 2016, pp. 1–6.

[27] B. Li, H. Kumar, and A. P. Petropulu, "A joint design approach for spectrum sharing between radar and communication systems," in *2016 IEEE International Conference on Acoustics, Speech and Signal Processing (ICASSP)*, March 2016, pp. 3306–3310.

[28] B. Li, A. P. Petropulu, and W. Trappe, "Optimum Co-Design for Spectrum Sharing between Matrix Completion Based MIMO Radars and a MIMO Communication System," *IEEE Transactions on Signal Processing*, vol. 64, no. 17, pp. 4562–4575, September 2016.

[29] D. W. Bliss, "Cooperative radar and communications signaling: The estimation and information theory odd couple," in *2014 IEEE Radar Conference*, May 2014, pp. 0050–0055.

[30] M. Bica and V. Koivunen, "Delay estimation method for coexisting radar and wireless communication systems," in *2017 IEEE Radar Conference (RadarConf)*, May 2017, pp. 1557–1561.

[31] Y. Yang and R. Blum, "MIMO radar waveform design based on mutual information and minimum mean-square error estimation," *IEEE Transactions on Aerospace and Electronic Systems*, vol. 43, no. 1, pp. 330–343, January 2007.

[32] J. A. del Peral-Rosado, J. A. López-Salcedo, G. Seco-Granados, F. Zanier, and M. Crisci, "Joint maximum likelihood time-delay estimation for LTE positioning in multipath channels," *EURASIP Journal on Advances in Signal Processing*, vol. 2014, no. 1, p. 33, Mar 2014.

[33] A. R. Chiriyath, B. Paul, G. M. Jacyna, and D. W. Bliss, "Inner Bounds on Performance of Radar and Communications Co-Existence," *IEEE Transactions on Signal Processing*, vol. 64, no. 2, pp. 464–474, January 2016.

[34] P. Comon and C. Jutten, *Handbook of Blind Source Separation: Independent component analysis and applications*. Academic Press, 2010.

[35] N. Levanon, "Multifrequency radar signals," in *Record of the IEEE 2000 International Radar Conference*, 2000, pp. 683–688.

[36] G. Lellouch, P. Tran, R. Pribic, and P. van Genderen, "OFDM waveforms for frequency agility and opportunities for Doppler processing in radar," in *Proceedings of IEEE Radar Conference*, May 2008, pp. 1–6.

[37] S. Sen and A. Nehorai, "Adaptive design of OFDM radar signal with improved wideband ambiguity function," *IEEE Transactions on Signal Processing*, vol. 58, no. 2, pp. 928–933, February 2010.

[38] M. Bică and V. Koivunen, "Generalized Multicarrier Radar: Models and Performance," *IEEE Transactions on Signal Processing*, vol. 64, no. 17, pp. 4389–4402, September 2016.

[39] C. Sturm and W. Wiesbeck, "Waveform Design and Signal Processing Aspects for Fusion of Wireless Communications and Radar Sensing," *Proceedings of the IEEE*, vol. 99, no. 7, pp. 1236–1259, July 2011.

[40] W. Wiesbeck, L. Sit, M. Younis, T. Rommel, G. Krieger, and A. Moreira, "Radar 2020: The future of radar systems," in *2015 IEEE International Geoscience and Remote Sensing Symposium (IGARSS)*, July 2015, pp. 188–191.

[41] C. Sturm, T. Zwick, W. Wiesbeck, and M. Braun, "Performance verification of symbol-based OFDM radar processing," in *Proceedings of IEEE Radar Conference*, May 2010, pp. 60–63.

[42] M. Braun, C. Sturm, and F. K. Jondral, "On the single-target accuracy of ofdm radar algorithms," in *2011 IEEE 22nd International Symposium on Personal, Indoor and Mobile Radio Communications*, Sept 2011, pp. 794–798.
[43] R. F. Tigrek, W. J. A. D. Heij, and P. V. Genderen, "OFDM Signals as the Radar Waveform to Solve Doppler Ambiguity," *IEEE Transactions on Aerospace and Electronic Systems*, vol. 48, no. 1, pp. 130–143, January 2012.
[44] M. C. Jackson, "The geometry of bistatic radar systems," *Communications, Radar and Signal Processing, IEE Proceedings F*, vol. 133, no. 7, pp. 604–612, December 1986.
[45] S. Haykin, "Cognitive radar: a way of the future," *IEEE Signal Processing Magazine*, vol. 23, no. 1, pp. 30–40, January 2006.
[46] L. Giugno and M. Luise, "Optimum pulse shaping for delay estimation in satellite positioning," in *2005 13th European Signal Processing Conference*, September 2005, pp. 1–6.
[47] F. Zanier and M. Luise, "Fundamental issues in time-delay estimation of multicarrier signals with applications to next-generation GNSS," in *2008 10th International Workshop on Signal Processing for Space Communications*, October 2008, pp. 1–8.
[48] F. Zanier, G. Bacci, and M. Luise, "Criteria to Improve Time-Delay Estimation of Spread Spectrum Signals in Satellite Positioning," *IEEE Journal of Selected Topics in Signal Processing*, vol. 3, no. 5, pp. 748–763, October 2009.
[49] S. M. Kay, *Fundamentals of Statistical Signal Processing: Estimation Theory*. Upper Saddle River, NJ, USA: Prentice-Hall, Inc., 1993.

Marian Bică (S'15–M'18) was born in Romania in 1985. He received the B.Sc. degree in telecommunications from the "Politehnica" University of Bucharest, Romania, in 2009, the M.Sc. (Tech.) degree in communications engineering and the D.Sc. (Tech.) degree in signal processing technology from Aalto University (former Helsinki University of Technology), Finland, in 2012 and 2018 respectively.

He has been with the Department of Signal Processing and Acoustics, Aalto University, since 2010. From 2010 to 2012 as a Research Assistant, from 2013 to 2018 as a Doctoral Candidate and since 2018 as a Postdoctoral Researcher. From November 2014 to May 2015 he has been a Visiting Scholar at the University of Southern California (USC), Los Angeles, CA. His research interests include radar, communications and statistical signal processing, information theory, multicarrier systems, as well as cognitive systems and machine learning.

Visa Koivunen (M'87–SM'98–F'11) received his D.Sc. (EE) degree with honors from the University of Oulu, Dept. of Electrical Engineering. Years 1991-1995 he was a visiting researcher at the Univ of Pennsylvania, Philadelphia, USA. Since 1999 he has been a full Professor of Signal Processing at Aalto University (Helsinki UT), Finland. He received the Academy professor position. Years 2003-2006 he was also adjunct full professor at the University of Pennsylvania, Philadelphia, USA. During his sabbatical term in 2006-2007 he was a visiting fellow at Princeton University, NJ, USA. He was part-time Visiting Fellow at Nokia Research (2006-2012). Since 2010 he has been part time visiting fellow and spent sabbaticals at Princeton University.

Dr. Koivunen's research interest include statistical, communications, radar, multisensor system signal processing. He has published more than 400 papers in international scientific conferences and journals and holds 6 patents. He co-authored multiple papers receiving the best paper award in IEEE and other conferences. He was awarded the IEEE Signal Processing Society best paper award for the year 2007 (with J. Eriksson) and 2017 (w Zoubir, Muma and Chakhchouk). He served in editorial board for IEEE Signal Processing Letters, IEEE TR on Signal Processing, and IEEE Signal Processing Magazine. He was awarded the 2015 EURASIP (European Association for Signal Processing) Technical Achievement Award for fundamental contributions to statistical signal processing and its applications in wireless communications, radar and related fields. He is a member of the IEEE SPS Fellow Reference committee. He served as IEEE Signal Processing Society Distinguished Lecturer in 2015-2016. He was the general chair of 2018 Asilomar Conference.